PharmaSat: Drug dose response in microgravity from a free-flying integrated biofluidic/optical culture-and-analysis satellite

Antonio J. Ricco,[*a] Macarena Parra,[a] David Niesel,[b] Matthew Piccini,[a] Diana Ly,[a] Michael McGinnis,[b] Andrzej Kudlicki,[b] John W. Hines,[a] Linda Timucin,[a] Chris Beasley,[a] Robert Ricks,[a] Michael McIntyre,[a] Charlie Friedericks,[a] Michael Henschke,[a] Ricky Leung,[a] Millan Diaz-Aguado,[a] Christopher Kitts,[c] Ignacio Mas,[c] Mike Rasay,[c] Elwood Agasid,[a] Ed Luzzi,[a] Karolyn Ronzano,[a] David Squires,[a] Bruce Yost[a]

[a]NASA Ames Research Center, Moffett Field, CA, USA 94035;
[b]University of Texas Medical Branch, Galveston, TX, USA 77555;
[c]Santa Clara University, Santa Clara, California, USA 95053

ABSTRACT

We designed, built, tested, space-qualified, launched, and collected telemetered data from low Earth orbit from PharmaSat, a 5.1-kg free flying "nanosatellite" that supported microbial growth in 48 microfluidic wells, dosed microbes with multiple concentrations of a pharmaceutical agent, and monitored microbial growth and metabolic activity using a dedicated 3-color optical absorbance system at each microwell. The PharmaSat nanosatellite comprised a structure approximately 10 x 10 x 35 cm, including triple-junction solar cells, bidirectional communications, power-generation and energy-storage system, and a sealed payload 1.2-L containment vessel that housed the biological organisms along with the fluidic, optical, thermal, sensor, and electronic subsystems. Growth curves for *S. cerevisiae* (Brewer's yeast) were obtained for multiple concentrations of the antifungal drug voriconazole in the microgravity conditions of low Earth orbit. Corresponding terrestrial control experiments were conducted for comparison.

Keywords: PharmaSat, integrated microsystem, yeast, microfluidics, optical absorbance, voriconazole, nanosatellite

1. INTRODUCTION

1.1 Biology in outer space

Long-term spaceflight affects living organisms. Results for mammals are consistent with immune stress, decreased bone density, muscle atrophy, and slowed wound healing. For cells and microorganisms in culture, one consequence of microgravity is that thermal gradients do not cause convection due to thermally-induced fluid density differences, as is the case with Earth gravity; this can alter mass transport and thereby influence nutrient delivery and waste removal. For all living organisms, rates of damage from high-energy radiation increase measurably outside the shielding of Earth's magnetosphere (beyond ~ 65,000 km on the sunward side of Earth). Even in low Earth orbit (~ 160 – 2000 km), the trapped radiation belts result in higher radiation fluxes than on Earth's surface. For the short-duration PharmaSat experiment, mutation effects from radiation would be minimal. For microbes, rates and extent of growth vary in space due to microgravity effects, and even pathogen virulence has been reported to change.[1] As dramatized in the movie Apollo 13, astronauts during spaceflight can contract bacterial infections. Astronauts in space have also experienced infections with other opportunistic and pathogenic microbes. Effective treatment of bacterial infections has required therapy customized for the space environment, as evidence has accumulated that microbes respond differently to antimicrobials in the space environment. The PharmaSat experiment was focused on directly documenting alterations in antimicrobial resistance in the space environment using a well defined microbial system - the yeast, *S. cerevisiae*.

Integrated bioreactors have flown on manned spacecraft;[2-4] they require humans to initiate experiments, record data, and collect or prepare samples to return them to Earth for characterization.[2] Fully autonomous microsystems[5] like PharmaSat reduce the cost and obviate other limitations of human-tended space biological experiments, while expanding significantly the number of launch opportunities.

[*]ajricco@stanford.edu; phone 1 650 604 4276; fax 1 208 545 1231; www.nasa.gov/pharmasat/

Microfluidics, BioMEMS, and Medical Microsystems IX, edited by Holger Becker, Bonnie L. Gray, Proc. of SPIE Vol. 7929, 79290T · © 2011 SPIE · CCC code: 0277-786X/11/$18 · doi: 10.1117/12.881082

PharmaSat was developed to conduct low-cost, *in-situ*, outer-space studies of the efficacy of pharmaceutical agents against microbial pathogens or model organisms representative of these infectious agents. The PharmaSat space experiment tested a widely-used antifungal (AF) drug, voriconazole, against a common, well-studied "model" fungus, *Saccharomyces cerevisiae* (Brewer's yeast).

1.2 PharmaSat mission overview

On May 19, 2009, the 5.1-kg PharmaSat spacecraft launched from Wallops Flight Facility, Virginia, USA as a secondary payload aboard a Minotaur I rocket, whose primary payload was a US Air Force reconnaissance satellite, TacSat-3. This "hitchhiker" approach to placing science instruments in outer space offers much lower launch costs (~ $30,000 – $40,000/kg) than dedicated space biology missions, but can add operational constraints: PharmaSat had to be fully integrated and delivered for test and launch-vehicle integration more than 6 weeks prior to launch, and no power was available for thermal control prior to deployment in space (nevertheless, temperature was maintained near room temperature in a range specified as 4 – 37 °C in the launch facilities prior to flight). As an add-on payload, PharmaSat was mounted, using a vibration-damping fastener, to the Minotaur I upper-stage rocket motor; calculations predicted < 5 °C temperature increase inside the vessel containing the bio-fluidic subsystem, microbes, and pharmaceutical compound during the short burn time of this motor.

At 20 minutes post-launch, PharmaSat was spring-ejected from its so-call PPOD (poly-picosatellite orbital deployer[6]) into low-Earth orbit at 460 km elevation and 40° inclination as a free-flying autonomous satellite. It functioned nominally and within days, results from the drug-dose-dependence experiment were telemetered to Earth (http://www.nasa.gov/mission_pages/smallsats/pharmasat/main/index.html). Leveraging multiple micro and miniature technologies, PharmaSat is the first fully autonomous outer-space pharmaceutical dose-response analytical system. Here, we report the design and development of PharmaSat, along with preliminary spaceflight and ground-control experimental results from this integrated bio-fluidic/optical/thermal system.

2. DESIGN AND DEVELOPMENT

PharmaSat's 5.1 kg mass comprises a structure roughly 10 x 10 x 35 cm, Figure 1, including triple-junction solar cells; patch antenna for 2.4-GHz bidirectional communication using a commercial WiFi-technology radio; self-deploying omnidirectional "beacon" antenna for spacecraft location and education-and-outreach broadcasting on the amateur ("ham") band (437.465 MHz); mechanical structure; spacecraft power/processor/communications/control system (collectively, the "bus"); and the experiment containment vessel, internal volume 1.2 L (Figures 1, 2), which houses the bio/fluidic, optical, thermal, sensor, and payload electronics subsystems (Figure 2). Magnetic rods passively orient the satellite, aiming the spacecraft's long axis and hence the patch antenna towards Earth's north magnetic pole during the part of each 95-minute orbital period when the spacecraft is above the northern hemisphere. Magnetic hysteresis rods damp nutation or "wobble" in spacecraft motion by dissipating energy as heat when they move across Earth's magnetic field lines.

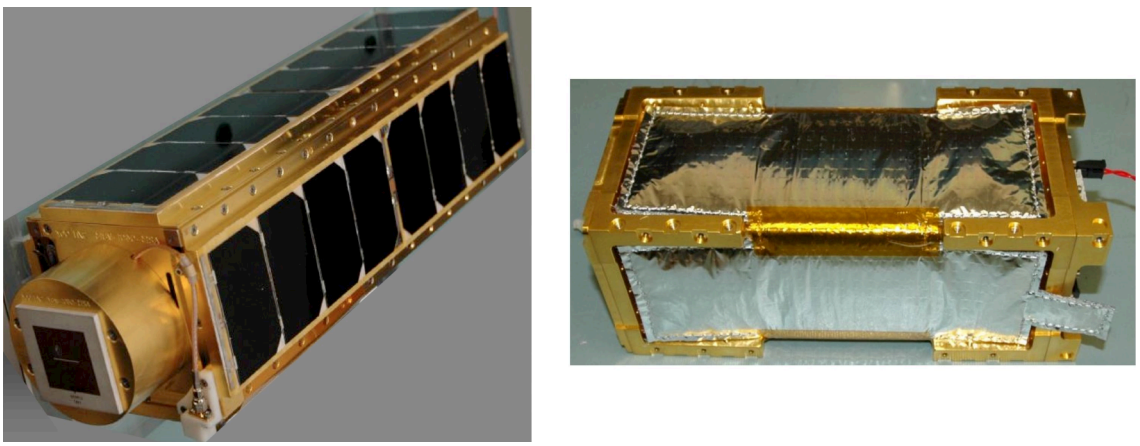

Figure 1. Integrated PharmaSat free-flying satellite (~35 cm long, 5.1 kg) with solar panels, patch antenna on near end (*left*); payload frame and insulation-wrapped containment vessel (*right*) containing the integrated culturing and bioanalytical system.

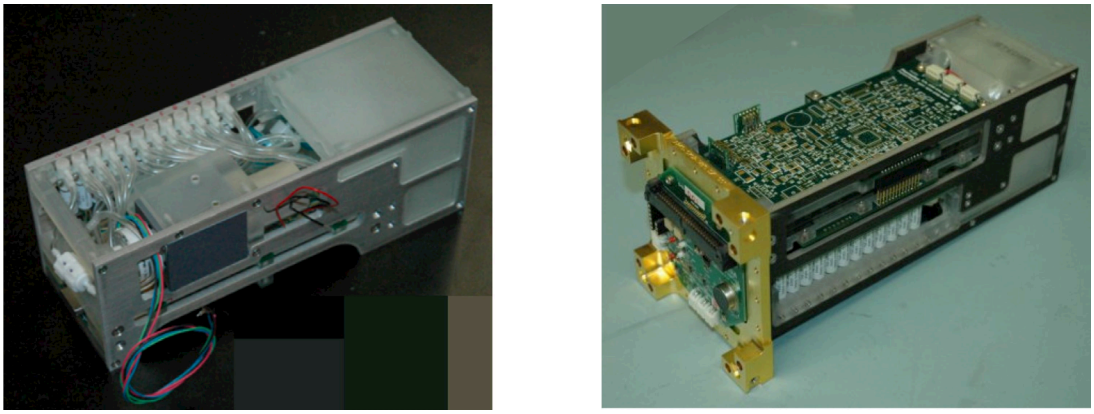

Figure 2. Two views of PharmaSat integrated payload (which slides inside the pressure vessel shown in Figure 1). It includes fluidic, optical, thermal, sensor, and electronics subsystems.

2.1 Fluidic subsystem

The PharmaSat fluidic system (cross section: Figure 3) includes forty-eight 100-µL culture wells, each 4 mm in diameter x 7.8 mm deep, and 11 solid-state reference wells containing a variety of colored polymer absorbance standards. Use of 9-mm pitch along the rows and 9- and 13.5-mm center-to-center row spacing allows fluidic card optical analysis with standard multiwell plate readers. The fluidic card was fabricated by Micronics, Inc. from laser-cut poly(methylmethacrylate) layers (Figure 4) laminated to one another using pressure-sensitive acrylic adhesive interlayers supported on PET (poly(ethylene terephthalate)) carrier films. Four independent sets of manifolded fluidic inlets and outlets supply nutrients and antifungal agent to the four 12-well banks. Yeast cells are confined in the microwells by integral 1.2-µm pore-size nylon fiber membrane filters (Sterlitech).

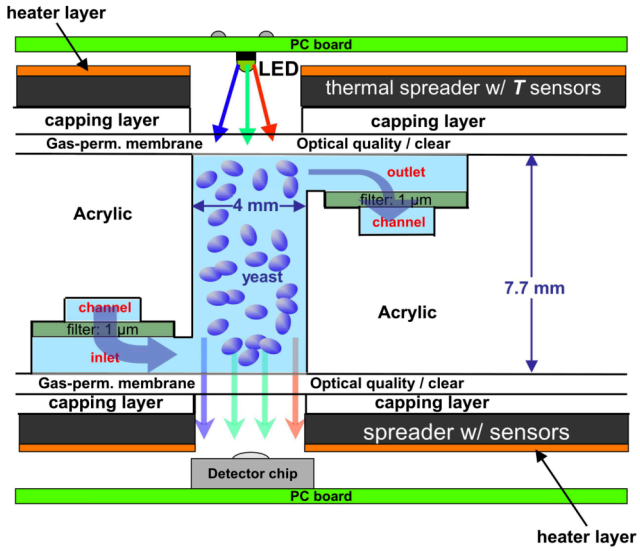

Figure 3. Microfluidic, optical, and thermal cross section of one of 48 wells; each contains 100 µL and has integral 1.2-µm filter membranes at inlet and outlet to confine the yeast. RGB LED and detector pair at opposite ends of each well measure 3-color transmittance. Patterned Kapton heaters plus aluminum thermal spreaders give ± 0.5 °C temperature uniformity across the card.

Covering the tops and bottoms of the fluidic cards is a 51-µm-thick layer of optical-quality poly(styrene) (PS), which provides gas permeability for CO_2 and O_2 exchange and optical transparency for 3-color absorbance measurements. Cards were initially fabricated without a top cover layer, sterilized using ethylene oxide, off-gassed in vacuum for 2 weeks at 55 °C, and stored in sterile bags prior to filling.

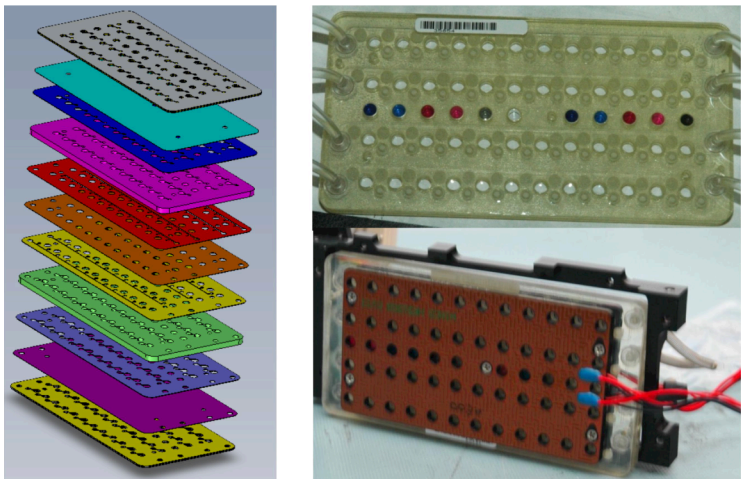

Figure 4. Exploded view of fluidic card showing laser-cut acrylic and PSA layer stack (left). Completed card (upper right) shows 4 banks of 12 wells each and 11 reference wells (colored, along center line). A pair of patterned Kapton heater films with aluminum spreader plates (bottom) sandwiches the fluidic card.

Inoculation of biowells with microorganisms and fluid filling of fluid storage bags, tubing, channels, and wells were carried out under sterile conditions prior to payload integration. To prepare a card for laboratory or flight experiments, solid-state colored optical reference elements were placed in the eleven "dry" wells. Each biowell was then inoculated with 10 µL of dormant *S. cerevisiae* culture (in distilled water), to provide a final density of 5 – 10 x 10^5 organisms/mL, with care to avoid wetting the filter membranes. To help eliminate gas bubbles, wells and channels were purged with CO_2. The open wells were then covered by a second PS film. Channels and inoculated biowells were next filled with thoroughly vacuum-degassed sterile water; any remaining CO_2 bubbles dissolved gradually as stasis medium flowed through the wells and channels.

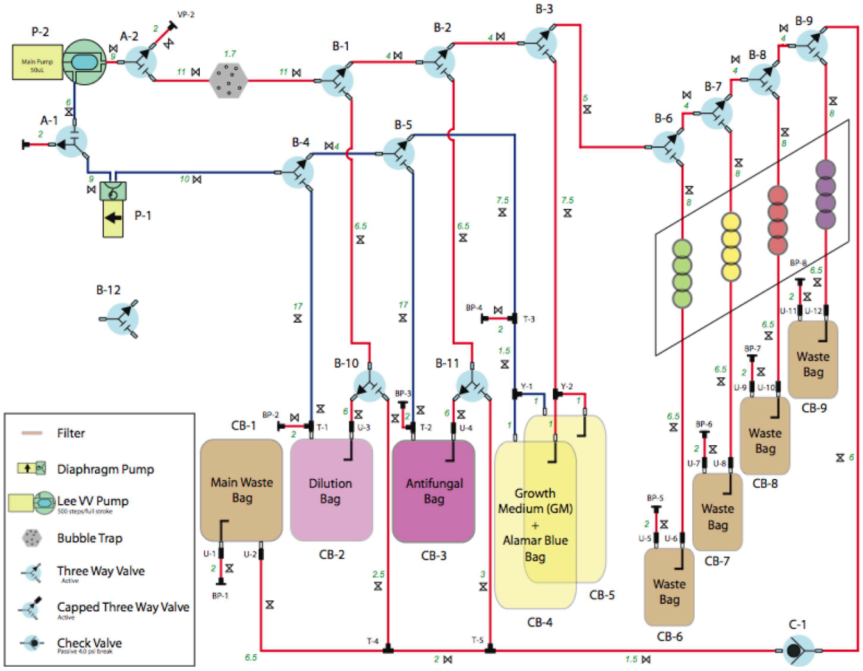

Figure 5. Block diagram of fluid delivery and dosing system. The variable-volume (VV) metering pump makes precise dilutions of the antifungal agent for delivery at 3 concentrations. The diaphragm pump provides higher flow rates for circulation and mixing. Each bank of 12 wells has a dedicated waste bag, while the growth medium, antifungal agent, dilution, and mixing bags are common.

The fluid-delivery-and-dosing system, Figure 5, comprises 14 solenoid-operated valves (The Lee Co.); a piston-type metering pump (Lee) and a diaphragm-based pump (KNF Neuberger); a bubble trap (developed in-house); nine medical-grade fluoropolymer bags (American Fluoroseal) for growth medium, AB viability dye, antifungal agent, and waste; and medical-grade connecting tubing (Sanipure 60, Saint-Gobain Performance Plastics). The fluidic system supports organism dormancy during the pre-flight, launch, and deployment period; it supplies growth medium to initiate organism growth upon attainment of stable orbit; and it mixes, meters, and supplies the antifungal agent, voriconazole, at three concentrations. The fluidics card and system maintain the micro-wells in a bubble-free state for at least 7 weeks after loading and assembly, despite the permeability of the covering membranes to water vapor. This immunity to bubble formation is conferred by filling the waste bag for each well bank with several mL of stasis buffer maintained at a low "back pressure", thereby replacing water lost to evaporation to prevent bubble formation. Evaporation was also mitigated by containment of the fluidic card within the viton-o-ring-sealed pressure vessel, the internal unoccupied air volume (< 0.4 L) of which was humidified to near saturation by evaporation through the PS cover films of the fluidic card.

2.2 Optical, thermal, and sensor subsystems

Each of the 48 fluidic and 11 solid-state reference wells has a dedicated optical sub-assembly (Figure 3), comprised of a 3-color LED (Lite-On) providing illumination bands centered at 470, 525, and 615 nm with 26, 35, and 18 nm spectral half-widths, respectively, along with an intensity-to-frequency integrated detector (Texas Advanced Optoelectronic Solutions TSL230BR) providing more than five decades of linear digital output with frequency being proportional to light intensity. Only a single LED wavelength band at one well is energized at a time, eliminating any possibility of optical crosstalk.

The optical system tracks organism growth in two ways: optical density changes due to light scattering by the yeast cells, which is directly proportional to cell number,[7] and color change of a "viability dye," alamar blue (AB, Invitrogen), which is deliberately added to the growth medium. AB changes from blue (the oxidized form) to pink (the reduced form) when enzymes generated by cellular metabolic processes act upon it.[8] AB's blue form has its absorbance maximum at 600 nm, the pink at 570 nm. To first order, the red LED tracks the concentration of oxidized AB, the green is sensitive to the pink form, and the blue, where neither pink nor blue forms of the dye absorbs strongly, responds mainly to light scattering by the yeast cells, i.e. turbidity.

The match of the three LED bands to the three optical parameters of interest is imperfect. We measured optical absorbance "cross terms", finding the three most important of them to be (1) absorption of the blue band by the blue form of AB (10% of its absorbance at 615 nm); (2) absorption of the blue band by the pink form of AB (29% of its absorbance at 525 nm); (3) absorption of the green band by the blue form of AB (35% of its absorbance at 615 nm). Figure 6 shows uncorrected absorbances (top) and absorbances after correction for the optical cross terms (bottom) for the laboratory growth of *S. cerevisiae* in one well of the fluidics card. This correction allows for reasonably accurate estimation of cell number and concentrations of AB in its oxidized and reduced forms.

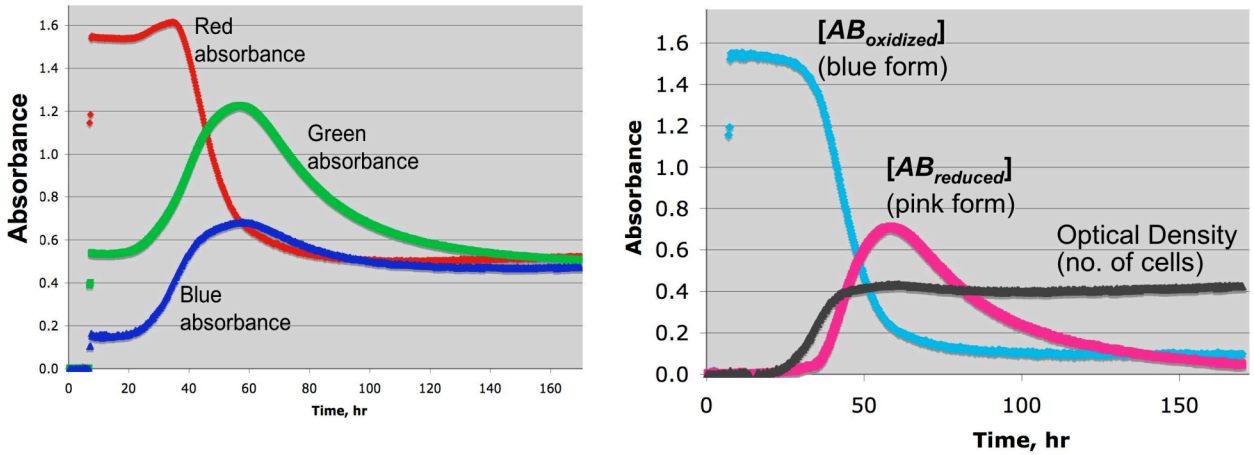

Figure 6. Three-color absorbance of one microwell of growing yeast measured with the PharmaSat optical system. *Left*: As-measured absorbances, corrected for known absorbance of initial concentration of blue form of alamar blue. *Right*: Absorbances after correction for "cross terms", resulting in absorbances of the two forms of AB and the optical density due to light scattering by the yeast cells.

The thermal system utilizes a pair of custom Kapton-film, patterned nichrome trace heaters (Minco) adhered to 3-mm-thick black-anodized Al plates (minimizing light reflections) that serve as thermal spreaders and that sandwich the fluidic card (Figure 3) to provide thermal uniformity. Closed-loop thermal control is provided via the system microcontroller, providing temperature stability of < 0.3 °C. Average power consumption by the thermal systems was ~ 2 W to maintain the fluidic card at the 27 °C growth temperature of yeast during the experiment in orbit.

Sensors in the containment vessel include six for temperature (Analog Devices AD590) distributed over the thermal spreaders to monitor fluidic card temperature and to provide the feedback control signal; a micromachined pressure transducer (Motorola MPXH6101A); and a thin-film capacitive humidity sensor (Sensirion SHT15). In the spacecraft bus, temperature is monitored by additional AD590's and a PIN diode (Hamamatsu S3071) monitors radiation flux.

3. PRELIMINARY RESULTS

Figure 7 shows the operational timeline for the PharmaSat space experiment. Nearly 7 weeks after integration with the rocket, PharmaSat launched on May 19, 2009 from Wallops Flight Facility; it was deployed from the launch vehicle about 20 min later. Radio contact was established within hours and its orbit passively stabilized by the magnetic field-alignment and hysteresis rods. Orbital trajectory places PharmaSat in sunlight ~ 2/3 of the time and darkness ~ 1/3 of each 97-min orbit. Lithium-ion batteries in the bus are charged by the solar panels, providing uninterrupted power when the satellite is in darkness and allowing power draw to exceed solar panel output for limited time periods in sunlight.

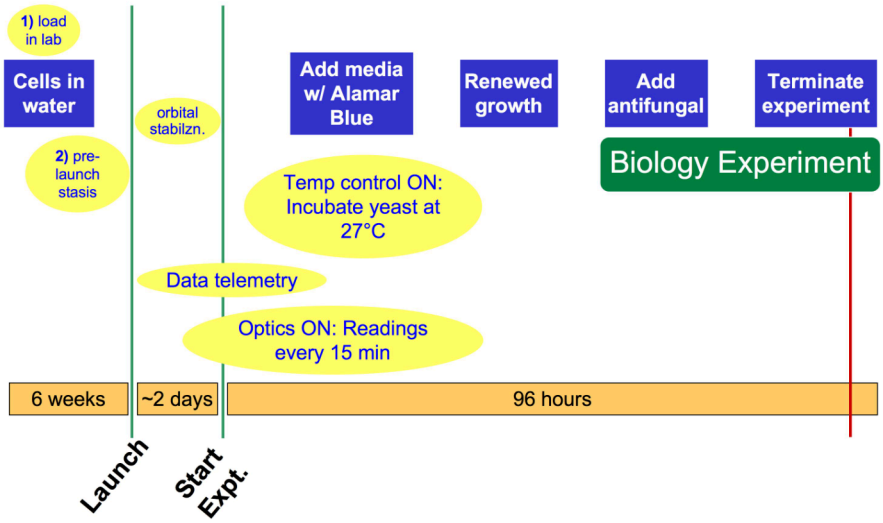

Figure 7. Operational timeline for PharmaSat space experiment.

The primary local motion of the satellite as it orbits the Earth is rotation about its long axis. Depending on the angular momentum imparted to the spacecraft upon deployment from the launch vehicle, its rotation rate is typically higher in the initial hours of the mission, slowing over the course of hours after deployment to a steady-state condition in which dissipation by the hysteresis rods is balanced by angular momentum imparted by movement through the changing magnetic field as it flies between the northern and southern hemispheres on each orbit. For nanosatellites, the size and mass of PharmaSat, this steady-state rotation rate is typically 1 – 2 rpm.

When the gravity aboard the satellite is calculated to be < 10^{-3} x Earth gravity—by evaluating time variations in currents from the four body-mounted solar panels as the satellite rotates them in and out of sunlight—the experiment can commence. Accordingly, some 47 hr after orbital deployment, the temperature of the PharmaSat fluidic card was changed by the autonomous onboard software from ambient (~ 6 – 16 °C) to a constant 27 °C (uniformity over the card estimated at ± 0.5 °C from multiple temperature sensors integrated with the card). Once the temperature stabilized, *S. cerevisiae* growth was initiated 3.6 hr later in four time-sequenced sets of 12 wells each. This was achieved by displacing the stasis medium via a 3x-volume exchange (~ 300 µL/well) of nutrient medium (RPMI-1640, prepared as reported elsewhere,[9] but omitting phenol red) that included alamar blue viability dye at 10% of its stock concentration.

The fluidics card locates the fluid entrance to each cylindrical well near one end of the cylinder; the exit is near the opposite end, approximately 180° around the well circumference from the entrance. Having the entrance and exit diagonally opposite one another is important because medium exchange is by diffusion only: the small thermal gradients that invariably exist in fluidic systems, even with well-controlled temperature, cause fluid density differences that, on Earth, can lead to gravity-driven fluid movement, which often hastens the mixing process. In milli- or micro-gravity, however, fluid density differences do not cause fluid movement—colder, denser fluid does not "sink." Thus, creating a flow path that traverses the entire length and crosses the diameter of the cylindrical well helps minimize diffusion lengths, shortening mixing time. The 3x-volume exchange of nutrient for stasis medium occurs over a period of roughly one hour for each bank of 12 wells, with several periods of pumping alternating with periods of diffusive mixing. In this way, exchange of ~95% of the original stasis buffer is achieved in each well.

Meaningful measurements of antifungal dose dependence require the antifungal agent to be introduced when the yeast are growing stably but prior to the culture reaching high density, at which point the AF is ineffective. Because growth rate in the microgravity environment was not known in advance, growth progress aboard PharmaSat was monitored by telemetry; based on initial growth rates, a software command was uplinked to administer AF approximately 12 hr after initial RPMI growth medium introduction.

An identical satellite system, the flight spare, was housed in our ground laboratory inside a thermal chamber calibrated to mimic temperatures reported from the satellite; power was provided by a regulated power supply rather than solar cells. *S. cerevisiae* were loaded into the fluidic card of this control satellite from the same prepared cultures within two days of the flight loading of yeast. This "delayed synchronous" ground control experiment was conducted in order to meaningfully compare ground and space results.

Figure 8 shows the results from the ground-control experiment. Similar curves were obtained from the spaceflight experiment, but with differences in the average growth rates (see below). The data in Figure 8 are corrected absorbances of the oxidized (blue) form of AB throughout the growth and AF challenge process, measured using the red LED (615 nm), after correction for cross terms as described above. After initial growth, a growth medium-plus-antifungal mixture was pumped into the four 12-well banks at AF concentrations of 0 ("Control"), 0.13, 0.50, and 2.0 µg/mL. The minimum inhibitory concentration (MIC: the lowest concentration of AF that inhibits growth after overnight incubation) of voriconazole for *S. cerevisiae* was determined to be 0.5 µg/mL in ground laboratory studies conducted before the flight mission. Hence, we chose to test ¼x, 1x, and 4x the MIC, resulting in the varying inhibition of yeast growth shown in Figure 8 for the ground-control measurements. Each of the four AF concentrations (including zero) was tested with $n = 6$ independent microwells, which were initially loaded with yeast corresponding to an approximate optical density (OD) of 0.1. The remaining 6 wells of each bank of 12 were loaded with yeast at an OD of 0.2: in the event that insufficient organisms had survived the stasis period in the OD = 0.1 groups of wells, the OD = 0.2 wells would have provided an extra 100% population margin for initiating growth.

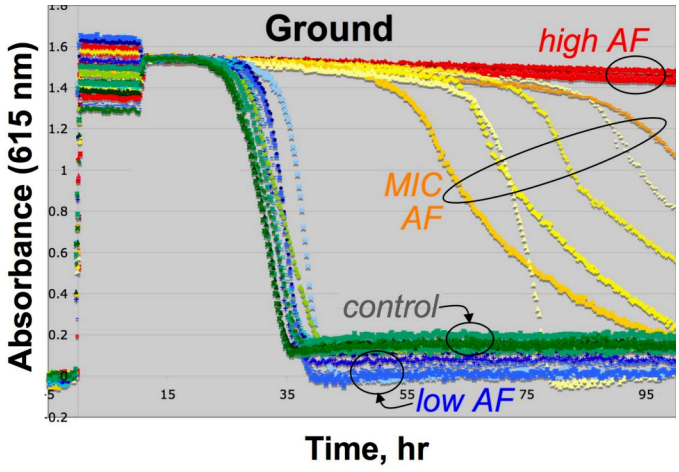

Figure 8. Terrestrial growth curves for *S. cerevisiae* at 27 °C in RPMI growth medium as a function of voriconazole antifungal concentration. 6 wells are tracked for each condition: "Control" includes no AF; "low AF", "MIC", and "high AF" correspond to 0.13, 0.50, and 2.0 µg/mL concentrations of voriconazole, respectively. (Circles and ellipses indicate sets of growth curves for each labeled condition).

Figure 9 analyzes AF = 0 yeast growth rates using the "lag time" before significant growth begins from two measurements: "metabolism" is based upon the loss of the blue form of AB, a consequence of metabolic activity; "cell division" is based upon increasing turbidity, which is proportional to cell population. The analysis indicates slower growth ($p \sim 0.03$) in the space microgravity environment than on Earth under normal gravity. In a significant gravitational field, even small thermal gradients, as might, for example, be caused by the on/off cycling of the fluidic card heater, can result in thermal convection in an otherwise quiescent culture. As explained above, in microgravity conditions fluid density differences do not drive convection. Thus, it may be the case that the yeast grow more slowly in space because the transport of nutrients to the cells and/or the transport of waste products away from the cells is slower, being driven solely by diffusion, compared to terrestrial experiments where (unintended) convection can play a role in mass transport.

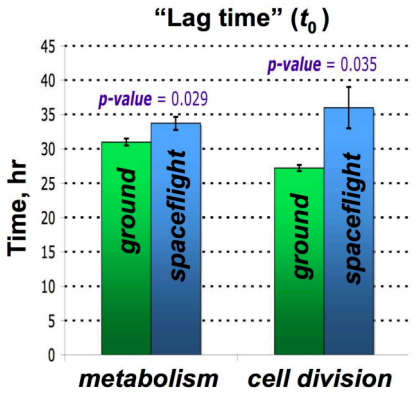

Figure 9. Comparison of "lag time" before yeast growth begins for ground and spaceflight measurements with zero antifungal agent concentration.

REFERENCES

[1] Wilson, J.W., Ott, C.M., Höner zu Bentrup, K., Ramamurthy, R., Quick, L., Porwollik, S., Cheng, P., McClelland, M., Tsaprailis, G., Radabaugh, T., Hunt, A., Fernandez, D., Richter, E., Shah, M., Kilcoyne, M., Joshi, L., Nelman-Gonzalez, M., Hing, S., Parra, M., Dumars, P., Norwood, K., Bober, R., Devich, J., Ruggles, A., Goulart, C., Rupert, M., Stodieck, L., Stafford, P., Catella, L., Schurr, M.J., Buchanan, K., Morici, L., McCracken, J., Allen, P., Baker-Coleman, C., Hammond, T., Vogel, J., Nelson, R., Pierson, D.L., Stefanyshyn-Piper, H.M., and Nickerson, C.A., "Space flight alters bacterial gene expression and virulence and reveals a role for global regulator Hfq," PNAS, 104, 16299-16304 (2007).

[2] Hammond, T.G., Lewis, F.C., Goodwin, T.J., Linnehan, R.M., Wolf, D.A., Hire, K.P., Campbell, W.C., Benes, E., O'Reilly, K.C., Globus, R.K., and Kaysen, J.H., "Gene expression in space," Nature Medicine, 5, 359 (1999).

[3] de Rooij, N.F., Gautsch, S., Briand, D., Marxer, C., Mileti, G., Noell, W., Shea, H., Staufer, U., and van der Schoot, B., "MEMS for space," Proc. Transducers 2009, IEEE: New York (2009); pp. 17-24.

[4] Cefai, J.J., Barrow, D.A., Woias, P. and Muller, E., "Integrated chemical analysis microsystems in space life sciences research," J. Micromech. Microeng., 4, 172 (1994).

[5] Ricco, A.J., Hines, J.W., Piccini, M., Parra, M., Timucin, L., Barker, V., Storment, C., Friedericks, C., Agasid, E., Beasley, C., Giovangrandi, L., Henschke, M., Kitts, C., Levine, L., Luzzi, E., Ly, D., Mas, I., Mclntyre, M., Oswell, D., Rasay, R., Ricks, R., Ronzano, K., Squires, D., Swaiss, G., Tucker, J., and Yost, B., "Autonomous genetic analysis system to study space effects on microorganisms: Results from orbit," Proc. Transducers 2007, IEEE: New York (2007); pp. 33-37.

[6] Puig-Suari, J., Turner, C., Ahlgren, W., "Development of the standard cubesat deployer and a cubesat class picosatellite," 2001 Aerospace Conference, IEEE Proceedings, 1/347-353 (2001).

[7] Ricco, A.J., Agasid, E., Barker, V., Fahlen, T., Hines, J.W., Levine, L., Mancinelli, R., Mrdjen, P., Oswell, D., Ricks, R., Ronzano, K. Squires, D., Storment, C., Swaiss, G., Timucin, L., Udoh, U., and Yost, B., "Integrated system to analyze the genetic effects of the space environment on living cells in culture: GeneSat," Proceedings μTAS 2005, Transducers Research Foundation: Cleveland (2005), pp. 527–529.

[8] O'Brien, J., Wilson, I., Orton, T., and Pognan, F., "Investigation of the alamar blue (resazurin) fluorescent dye for the assessment of mammalian cell cytotoxicity, Eur. J. Biochem., 267(17), 5421–5426 (2000).
[9] "Reference method for broth dilution antifungal susceptibility testing of yeasts. Approved standard M27-A2", 2nd ed. National Committee for Clinical Laboratory Standards, Villanova, PA (2002); Appendix A and Table 6.